Paper No. 1722. (quote when citing this article)
Eleventh World Conference on Earthquake Engineering
ISBN: 0 08 042822 3

COMPARISON OF BODY AND RAYLEIGH WAVE DISPLACEMENTS GENERATED BY A VERTICAL POINT FORCE ON A LAYERED ELASTIC MEDIUM

SHUJI TAMURA

Dept. of building engineering, Tokyo Institute of Technology, 2-12-1, O-okayama, Meguro-ku, Tokyo, 152, Japan

ABSTRACT

A numerical method is presented for determining the ground surface displacement induced by a vertical sinusoidal force on a three-dimensional layered elastic half-space. The contribution of the residue of the Rayleigh poles and the branch line integrals, i.e., that of Rayleigh and body waves, to the ground displacement is computed for two-layered and four-layered media. Its variation with S-wave velocity ratio of a two-layered medium, V_{S2}/V_{S1}, is examined. It is shown that, when V_{S2}/V_{S1} is less than 1.5 or when V_{S2}/V_{S1} is greater than 1.5 and the normalized frequency is less than 1, Rayleigh waves get to dominate as the normalized distance is greater than 3-4. When V_{S2}/V_{S1} is greater than 1.5 and normalized frequency is close to 1, body waves dominate up to a normalized distance of 100. The reason for this is found to be due to an extraordinary attenuation characteristics of body waves near the natural frequency of the medium. If a stiff surface layer overlying a soft layer, body waves also dominate in a high frequency range.

KEYWORDS

layered elastic half-space, vertical point force, displacement, Rayleigh wave, body wave, branch line integrals, normal mode solution

INTRODUCTION

After the pioneer work by Lamb (1904), Lamb's problem has been applied to the field of seismology. A vertical point force acting on the ground surface generates body and Rayleigh waves. The rigorous solution of the ground surface displacement is expressed as a sum of the branch line integrals and the residue of Rayleigh poles. The former corresponds to the contribution of body waves and the latter to that of Rayleigh waves. To evaluate the residue of Rayleigh poles is comparatively simple, while to evaluate the branch line integrals is complex. Therefore, Harkrider (1964) proposed "normal mode solution" in which the displacement is expressed as a sum of residue of Rayleigh poles only, neglecting the branch line integrals.

For a vertically oscillating source on the surface of a homogeneous, isotropic, elastic half space, Miller and Pursey (1955) showed that two thirds of the total energy goes to Rayleigh waves, while the remaining goes to body waves. In addition, the surface waves attenuate with a square root of distance, whereas the body waves attenuate with a square of distance along the surface (Ewing et al, 1957). Thus, Rayleigh waves become an order of magnitude greater than that of body waves if the distance from the source exceeds three times the wavelength (Saito, 1993).

In the case of a layered medium, however, most of methods for solving the ground surface displacement (e.g., Bouchon and Aki, 1977; Tajimi, 1980; Luco and Apsel, 1983) cannot distinguish body waves from Rayleigh waves. Therefore, it remains uncertain whether the body waves are actually neglected in a layered medium.

The object of this paper is to outline an analytical solution in which displacements of body and Rayleigh waves are separately determined, and to discuss whether the body waves are actually neglected in a layered medium.

THEORETICAL SOLUTIONS

Tokimatsu and Tamura (1995) presented an analytical solution of the ground surface displacement, of which outline is briefly described. The model considered consists of (N−1) layers overlying a half space as shown in Fig. 1a. Each layer is homogeneous, isotropic, and elastic. A vertical harmonic point source, $P_0\exp(-i\omega t)$, is assumed to be located on the ground surface of the z−axis as shown in Fig. 1b. Based on the Compound Matrix method (Saito and Kabasawa, 1993), such vertical and horizontal displacements, w and u, are defined by the wavenumber integral equations in the form

$$w(r,\omega) = \frac{1}{2\pi}\int_0^\infty \frac{P_0}{\omega c}\frac{Y_{14}}{Y_{24}} J_0(kr)kdk \tag{1}$$

$$u(r,\omega) = -\frac{1}{2\pi}\int_0^\infty \frac{P_0}{\omega c}\frac{Y_{12}}{Y_{24}} J_1(kr)kdk \tag{2}$$

in which $i=\sqrt{-1}$; k is the wavenumber; ω is the circular frequency; c is phase velocity (c=ω/k); r is distance from the source; Y_{12}, Y_{14}, and Y_{24} are variables in the Compound Matrix method; Y_{24} is equivalent to the characteristic equation for Rayleigh waves; and Y_{14}/Y_{24} and Y_{12}/Y_{24} are given by

$$\frac{Y_{14}}{Y_{24}} = \frac{i\left[(J_{13}-J_{23})(J_{31}-J_{41})-(J_{11}-J_{21})(J_{33}-J_{43})\right]c^2}{\left[(J_{12}-J_{22})(J_{31}-J_{41})-(J_{11}-J_{21})(J_{32}-J_{42})\right]} \tag{3}$$

$$\frac{Y_{12}}{Y_{24}} = \frac{\left[(J_{14}-J_{24})(J_{31}-J_{41})-(J_{11}-J_{21})(J_{34}-J_{44})\right]c^2}{\left[(J_{12}-J_{22})(J_{31}-J_{41})-(J_{11}-J_{21})(J_{32}-J_{42})\right]} \tag{4}$$

in which J_{ij} is the element of the matrix J defined by Haskell (1953). A potential difficulty in solving the above integrals is the presence of zero's of the denominator of the integrands. Based on the contour integration in a complex wavenumber plain shown in Fig. 2, Eqs. (1) and (2) can be rewritten as

$$w = \frac{i}{2}\sum_m \left[\frac{P_0 Y_{14}}{\omega c(\partial Y_{24}/\partial k)} kH_0^{(1)}(kr)\right]_{k=k_m} - \frac{1}{4\pi}\int_0^{\omega/V_{SN}} \frac{P_0}{\omega c}\left(\frac{Y_{14+}}{Y_{24+}} - \frac{Y_{14-}}{Y_{24-}}\right)H_0^{(1)}(kr)kdk - \frac{1}{4\pi}\int_0^{i\infty} \frac{P_0}{\omega c}\left(\frac{Y_{14-}}{Y_{24-}} - \frac{Y_{14+}}{Y_{24+}}\right)H_0^{(1)}(kr)kdk \tag{5}$$

$$u = -\frac{i}{2}\sum_m \left[\frac{P_0 Y_{12}}{\omega c(\partial Y_{24}/\partial k)} kH_1^{(1)}(kr)\right]_{k=k_m} + \frac{1}{4\pi}\int_0^{\omega/V_{SN}} \frac{P_0}{\omega c}\left(\frac{Y_{12+}}{Y_{24+}} - \frac{Y_{12-}}{Y_{24-}}\right)H_1^{(1)}(kr)kdk + \frac{1}{4\pi}\int_0^{i\infty} \frac{P_0}{\omega c}\left(\frac{Y_{12-}}{Y_{24-}} - \frac{Y_{12+}}{Y_{24+}}\right)H_1^{(1)}(kr)kdk \tag{6}$$

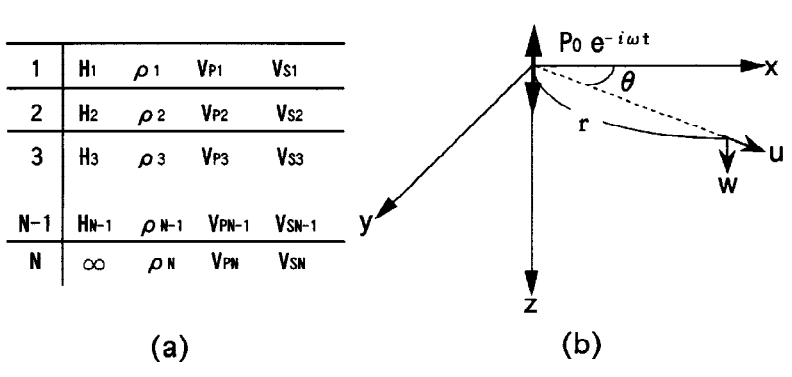

Fig. 1. Geometry of the multi-layered half space

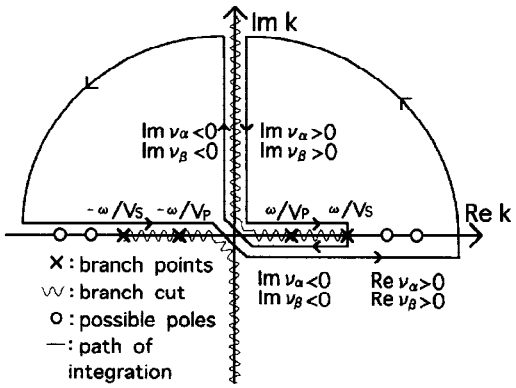

Fig. 2. Path of contour integration in complex wavenumber plane for Eqs. (1) and (2)

in which $H_0^{(1)}$ and $H_1^{(1)}$ are Hankel functions of the first kind of the order zero and one; k_m is the wavenumber of the mth mode; and subscripts + and − indicate that ν_α and ν_β defined by the following equations are positive and negative along the path of branch line integration.

$$\nu_\alpha^2 = k^2 - \omega^2/V_{PN}^2 \tag{7}$$

$$\nu_\beta^2 = k^2 - \omega^2/V_{SN}^2 \tag{8}$$

In each of Eqs. (5) and (6), the first term, w_r or u_r, corresponds to the contribution to the displacement of the residue of Rayleigh poles, i.e., the normal mode solution (Harkrider, 1964), and the second and third terms, w_{br} and u_{br}, w_{bi} and u_{bi}, correspond to the branch line integrals along the real and imaginary axes, respectively. Y_{14}/Y_{24} and Y_{12}/Y_{24} in the second term of Eqs. (5) and (6), have the following relations:

$$\frac{Y_{14+}}{Y_{24+}} = \left(\frac{Y_{14-}}{Y_{24-}}\right)^* \tag{9}$$

$$\frac{Y_{12+}}{Y_{24+}} = \left(\frac{Y_{12-}}{Y_{24-}}\right)^* \tag{10}$$

where * denotes complex conjugate. Y_{14}/Y_{24} and Y_{12}/Y_{24} in the third term of Eqs. (5) and (6), have the following relations:

$$\frac{Y_{14+}}{Y_{24+}} = -\left(\frac{Y_{14-}}{Y_{24-}}\right)^* \tag{11}$$

$$\frac{Y_{12+}}{Y_{24+}} = \left(\frac{Y_{12-}}{Y_{24-}}\right)^* \tag{12}$$

Substituting Eq. (9) into the second term of Eq. (5) yields

$$w_{br} = \frac{i}{2\pi}\int_0^{\omega/V_{SN}} \frac{P_0}{\omega c}\,\mathrm{Im}\left(\frac{Y_{14-}}{Y_{24-}}\right)H_0^{(1)}(kr)\,k\,dk \tag{13}$$

in which Im indicates the imaginary part of a complex number. Substituting Eq. (11) into the third term of Eq. (5) yields

$$w_{bi} = -\frac{1}{2\pi}\int_0^{i\infty} \frac{P_0}{\omega c}\,\mathrm{Re}\left(\frac{Y_{14-}}{Y_{24-}}\right)H_0^{(1)}(kr)\,k\,dk \tag{14}$$

in which Re indicates the real part of a complex number. Replacing k by ik in Eq. (14) leads to

$$w_{bi} = \frac{1}{\pi^2}\int_0^{\infty} \frac{P_0}{\omega c}\,\mathrm{Re}\left(\frac{Y_{14-}}{Y_{24-}}\right)K_0(kr)\,k\,dk \tag{15}$$

where K_0 is Bessel function of the second kind of order zero. The vertical displacement is then expressed as

$$w = \frac{i}{2}\sum_m \left[\frac{P_0 Y_{14}}{\omega c(\partial Y_{24}/\partial k)}\,kH_0^{(1)}(kr)\right]_{k=k_m} + \frac{i}{2\pi}\int_0^{\omega/V_{SN}} \frac{P_0}{\omega c}\,\mathrm{Im}\left(\frac{Y_{14-}}{Y_{24-}}\right)H_0^{(1)}(kr)\,k\,dk + \frac{1}{\pi^2}\int_0^{\infty} \frac{P_0}{\omega c}\,\mathrm{Re}\left(\frac{Y_{14-}}{Y_{24-}}\right)K_0(kr)\,k\,dk \tag{16}$$

Similarly, substitution of Eqs. (10) and (12) into Eq. (16) yields the horizontal displacement defined as

$$u = -\frac{i}{2}\sum_m \left[\frac{P_0 Y_{12}}{\omega c(\partial Y_{24}/\partial k)}\,kH_1^{(1)}(kr)\right]_{k=k_m} - \frac{i}{2\pi}\int_0^{\omega/V_{SN}} \frac{P_0}{\omega c}\,\mathrm{Im}\left(\frac{Y_{12-}}{Y_{24-}}\right)H_1^{(1)}(kr)\,k\,dk - \frac{1}{\pi^2}\int_0^{\infty} \frac{P_0}{\omega c}\,\mathrm{Im}\left(\frac{Y_{12-}}{Y_{24-}}\right)K_1(kr)\,k\,dk \tag{17}$$

where K_1 is Bessel function of the second kind of order one. In each of Eqs. (16) and (17), the first term corresponds to the amplitude of Rayleigh waves, w_r or u_r, and the second and third terms to the amplitude of body waves, w_b or u_b. The ground displacements expressed by Eqs. (16) and (17) can be numerically determined. It has been confirmed that the displacements computed by the present method agree with those presented by Saito (1993) for a half space.

Single Layer Overlaying an Elastic Half Space

The effects of various factors on the contribution of body and Rayleigh waves to the ground displacement are examined for two-layer models listed in Table 1. The factors considered include the distance from the source normalized by the wavelength of the fundamental Rayleigh mode; the frequency normalized by the

Table 1. Soil layer models

Layer No.	Thickness	Density	V_P	V_S			
				Model A	Model B	Model C	Model D
1	H	ρ	$3\,V_{S1}$	V_{S1}			
2	–	ρ	$3\,V_{S2}$	$1.2\,V_{S1}$	$1.5\,V_{S1}$	$3\,V_{S1}$	$6\,V_{S1}$

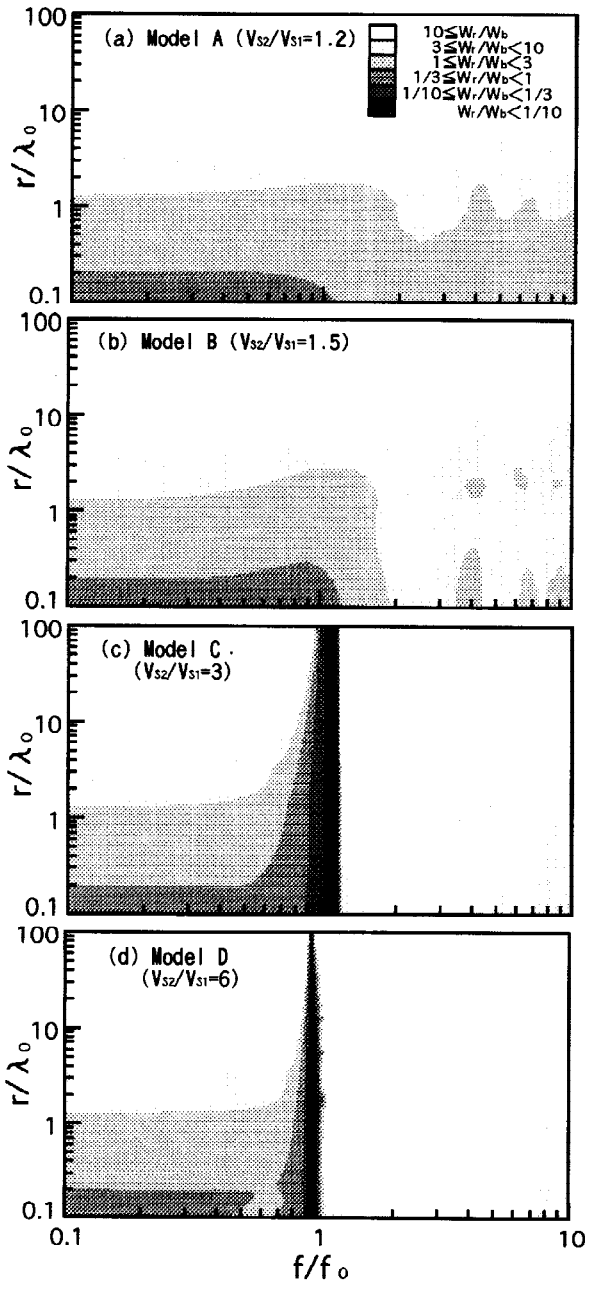

Fig. 3. Vertical amplitude ratios between body and Rayleigh waves with respect to dimensionless frequency, dimensionless distance, and V_{S2}/V_{S1}

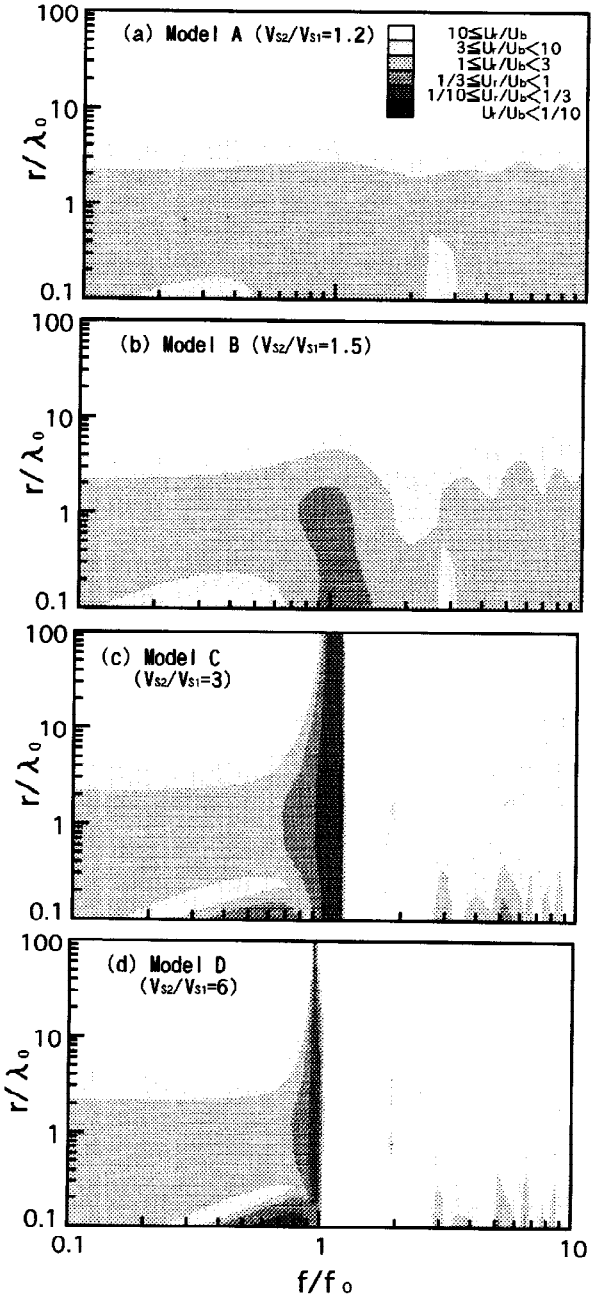

Fig. 4. Horizontal amplitude ratios between body and Rayleigh waves with respect to dimensionless frequency, dimensionless distance, and V_{S2}/V_{S1}

natural frequency, f/f_0, where $f_0=4H/V_{S1}$; and S-wave ratio between the surface layer and the half space, V_{S2}/V_{S1}. Figs. 3 and 4 show the amplitude ratio between body and Rayleigh waves with respect to dimensionless frequency and dimensionless distance, for vertical and horizontal components. When V_{S2}/V_{S1} is less than 1.5 or the normalized frequency is much less than 1, Rayleigh waves become one order of magnitude greater than that of body waves as the normalized distance is greater than 3–4. This is analogous to the characteristics of the propagating waves over a half space (Saito, 1993). In other cases, however, the trends are different. If V_{S2}/V_{S1} is greater than 1.5 and the normalized frequency is much more than 1, Rayleigh waves tend to dominate at closer source-to-sensor distance as the value of S-wave velocity ratio increases. If V_{S2}/V_{S1} is greater than 1.5 and the normalized frequency is close to 1, body waves dominate up to a normalized distance of 100.

To investigate why the body waves dominate at larger source-to-sensor distance near the natural frequency, the dimensionless displacements, $|w|$, $|w_r|$, and $|w_b|$, normalized by $P_0/(\rho V_{s1}{}^2 H)$, are plotted in Fig.5 against dimensionless distance at $f/f_0=0.2$, 1, 5 for Model C. At $f/f_0=0.2$, 5, as is the case of a half space, Rayleigh waves attenuate in proportion to $r^{-1/2}$, while body waves attenuate in proportion to r^{-2}. However, at $f/f_0=1$, body waves do not attenuate in proportion to r^{-2}, but show attenuation characteristics similar to Rayleigh waves, i.e., in proportion to $r^{-1/2}$. In addition, the body wave amplitude near the source is larger than that of Rayleigh waves. For this reason, If V_{S2}/V_{S1} is greater than 1.5 and normalized frequency is close to 1, body waves dominate up to a normalized distance of 100. In this case, the normal mode solution cannot work well. In other cases, the normal mode solution can work well, on the condition that the normalized distance is greater than 3–4.

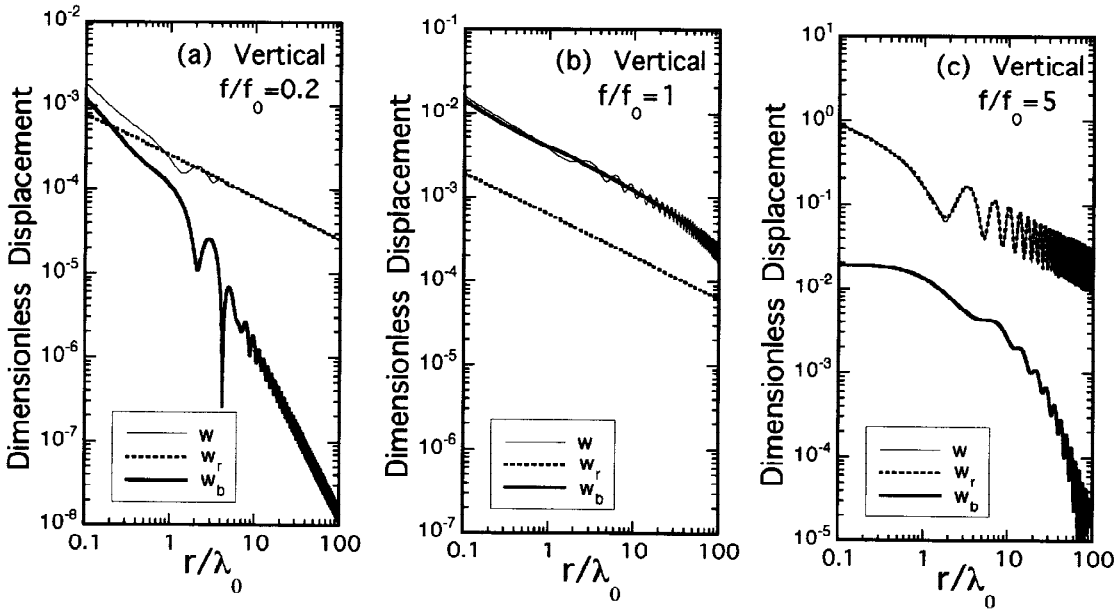

Fig. 5. Dimensionless displacement plotted against dimensionless distance with respect to f/f_0 for Model C

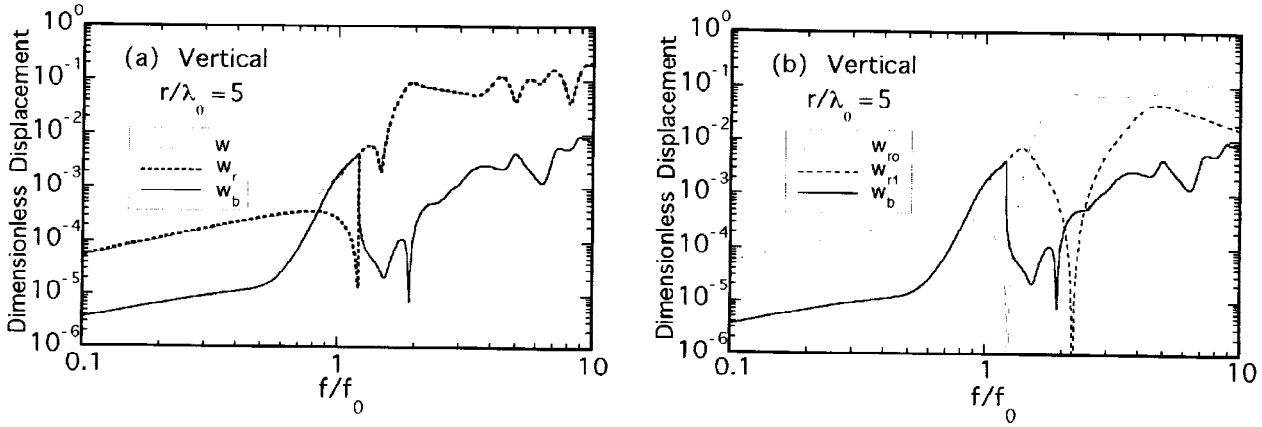

Fig. 6. Dimensionless displacement plotted against dimensionless frequency for Model C

In order to explain why the body waves attenuate in proportion to $r^{-1/2}$ at $f/f_0=1$, the dimensionless vertical displacement, w, w_r and w_b, are shown in Fig. 6a against dimensionless frequency for Model C. Fig. 6b shows the dimensionless displacement of the fundamental mode and the first higher mode Rayleigh waves, w_{r0} and w_{r1}, and that of body waves. At $f/f_0=1.2$, the amplitude of Rayleigh waves become a local minimum and that of body waves become a local maximum (Fig. 6a). However the amplitude of w changes smoothly at that frequency. The first higher mode is cut off at $f/f_0=1.2$ (Fig. 6b), where the amplitude of the first higher mode coincides with that of body wave. These findings suggest that the characteristics of Rayleigh and body waves are closely related with each other, when the normalized frequency is closed to 1. Thus, body wave shows attenuation characteristics similar to that of Rayleigh waves.

Multiple Layer Overlying an Elastic Half Space

The effects of presence of a stiff layer in a deposit on the propagation of body and Rayleigh waves are examined for four-layer models listed in Table 2. The stiffness of soil layers increases with depth in Model

Table 2. Soil layer models

Layer No.	Thickness H(m)	Density ρ (Mg/m^3)	V_P (m/s)	V_S (m/s) Model A	Model B	Model C
1	2	1.8	360	80	180	80
2	4	1.8	1000	120	120	180
3	8	1.8	1400	180	180	120
4	–	1.8	1400	360	360	360

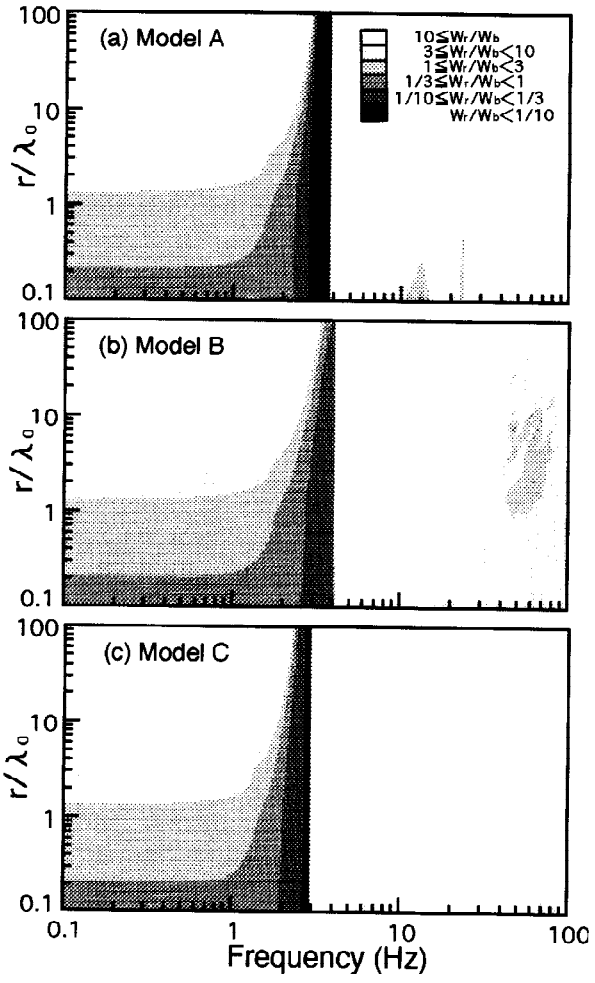

Fig. 7. Vertical amplitude ratios between body and Rayleigh waves with respect to frequency, dimensionless distance

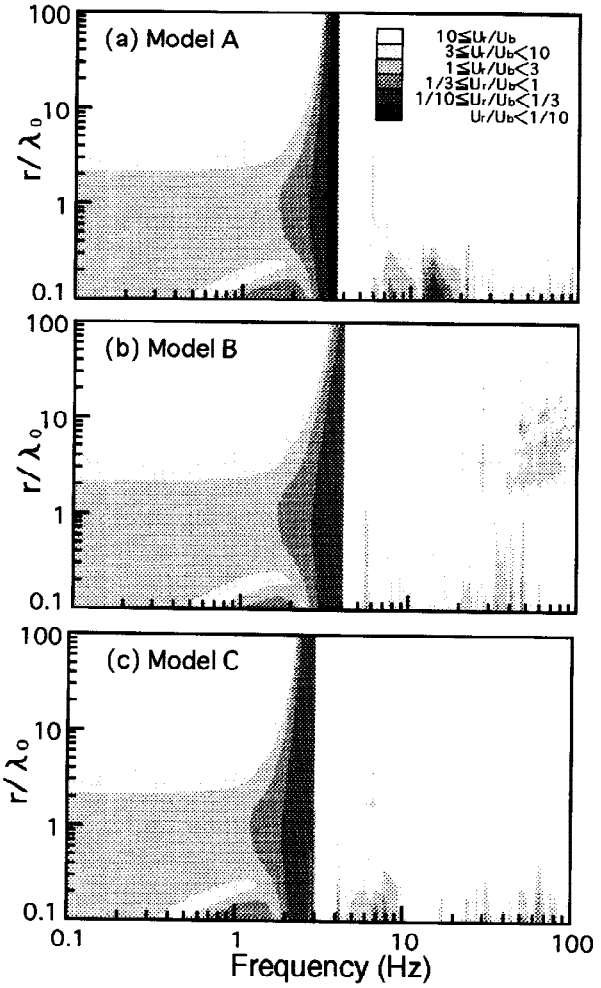

Fig. 8. Horizontal amplitude ratios between body and Rayleigh waves with respect to frequency, dimensionless distance

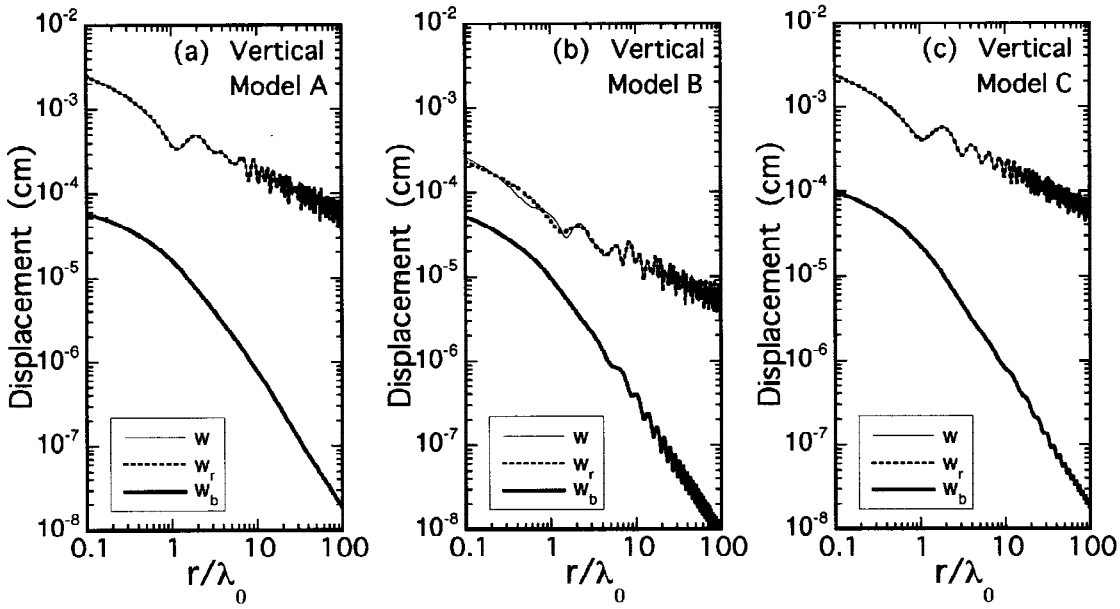

Fig. 9. Displacement plotted against dimensionless distance with respect to Model A–C for a force of 1kN

A, while the stiffness varies irregularly with depth in Models B and C; a stiff surface layer overlies a soft layer in Model B, and a stiff layer is sandwiched between soft layers in Model C. Figs.7 and 8 show the amplitude ratios between body and Rayleigh waves for vertical and horizontal components. The amplitude ratios between body and Rayleigh waves in Models A and C, show a trend similar to those of Models C and D shown in Figs. 3 and 4. By contrast, in the frequency range higher than 30Hz of Model B, Rayleigh waves dominate only when the normalized distance becomes greater than about 20.

In order to explain the above tendency, the vertical displacements of body and Rayleigh waves at 35Hz are shown in Fig. 9 against normalized frequency. In the case of Models A and C, Rayleigh waves amplitude near the source (r/λ_0=0.1) is 20–30 times that of body waves. By contrast, in the case of Model B, Rayleigh waves amplitude near the source is only 4 times that of body waves. Thus, in the case of Model B, Rayleigh waves dominate only when the normalized distance is greater than about 20.

CONCLUSIONS

A numerical method is presented for determining the ground surface displacement induced by a vertical sinusoidal force on a three-dimensional layered elastic half-space. The contribution of the residue of the Rayleigh poles and the branch line integrals, i.e., that of Rayleigh and body waves, to the ground displacement is computed and examined for two-layered and four-layered media.

In the case of a two-layered model:

1. When S-wave velocity ratio between the surface and base layers is less than 1.5 or when S-wave velocity ratio is greater than 1.5 and the normalized frequency is much less than 1, Rayleigh waves become one order of magnitude greater than that of body waves as the normalized distance is greater than 3–4. This is analogous to the characteristics of the propagating waves over a half space.
2. When S-wave velocity ratio between the surface and base layers is greater than 1.5 and the normalized frequency is much more than 1, Rayleigh waves tend to dominate at closer source-to-sensor distance, as the value of S-wave velocity ratio increases.
3. When S-wave velocity ratio between the surface and base layers is greater than 1.5 and the normalized frequency is close to 1, body waves dominate up to a normalized distance of 100. The reason for this is found to be due to an extraordinary attenuation characteristics of body waves at the natural frequency.

In the case of a four-layered model:

4. When a stiff surface layer overlying soft layer, Rayleigh waves in a high frequency range, dominate only when the normalized distance is greater than about 20.

REFERENCES

Bouchon, M. and Aki, K (1977). Discrete wave number representation of a seismic source wave fields, *Bulletin, Seismological Society of America*, **67(2)**, 259–277.

Ewing, W. M., Jardetzky, W. S., and Press, F (1957). Elastic waves in layered media, McGraw–Hill.

Harkrider, D. G. (1964). Surface waves in multilayered elastic media I. Rayleigh and Love waves from buried sources in a multilayered elastic half– space, *Bulletin, Seismological Society of America*, **54(2)**, 627–679.

Haskell, N. A. (1953). The dispersion of surface waves on multilayered media, *Bulletin, Seismological Society of America*, **43(1)**, 17–34.

Lamb, H. (1904). On the propagation of tremors over the surface of an elastic solid, *Phil. Trans. Soc. London,* **203**, Series A, 1–42.

Luco, J. E. and Apsel, R. J. (1983). On the green's functions for a layered half–space. I. , *Bulletin, Seismological Society of America*, **73(4)**, 909–929.

Miller, G. F. and Pursey, H. (1955). On the partition of energy between elastic waves in a semi–infinite solid, *Phil. Trans. Soc. London,* **233**, Series A, 55–69.

Saito, M. (1993). Branch line contribution in Lamb's problem, *Butsuri–Tansa,* **46(5)**, 372–380 (in Japanese).

Saito, M. and Kabasawa, H. (1993). Computations of reflectivity and surface wave dispersion curves for layered media II. Rayleigh wave calculations, *Butsuri–Tansa,* **46(4)**, 283–298 (in Japanese).

Tajimi, H. (1980). A contribution to theoretical prediction of dynamic stiffness of surface foundation, *Proc. of 7th WCEE*, Istanbul, Turkey, **5**, 105–112.

Tokimatsu, K. and Tamura, S. (1995). Contribution of Rayleigh and body waves to displacement induced by a vertical point force on a layered elastic half–space, *Journal of Structure and Construction Engineering, AIJ,* **476**, 95–101 (in Japanese).